Characterization of the interactions between Asp^{141} and Phe^{236} in the Mn^{2+}–L-malate binding of pigeon liver malic enzyme

Yen-I CHEN*, Yu-Hou CHEN*, Wei-Yuan CHOU* and Gu-Gang CHANG†[1]

*Graduate Institutes of Biochemistry and Life Sciences, National Defense Medical Center, Taipei 114, Taiwan, Republic of China, and †Faculty of Life Sciences, Institute of Biochemistry and Proteome Research Center, National Yang-Ming University, Taipei 112, Taiwan, Republic of China

The cytosolic malic enzyme from pigeon liver is very sensitive to the metal-catalysed oxidation systems. Our previous studies using the Cu^{2+}–ascorbate as the oxidation system showed that the enzyme was oxidized and cleaved at several positions, including Asp^{141}. The recently resolved crystal structure of pigeon liver malic enzyme revealed that Asp^{141} was near to the metal-binding site, but was not a direct metal ligand. However, Asp^{141} is located next to Phe^{236}, which directly follows the metal ligands Glu^{234} and Asp^{235}. Mutation at Asp^{141} caused a drastic effect on the metal-binding affinity of the enzyme. Since Asp^{141} and Phe^{236} are highly conserved in most species of malic enzyme, we used a double-mutant cycle to study the possible interactions between these two residues. Four single mutants [D141A (Asp^{141}→ Ala), D141N, F236A and F236L] and four double mutants (D141A/F236A, D141N/F236A, D141A/F236L and D141N/F236L), plus the wild-type enzyme were successfully cloned, expressed and purified to homogeneity. The secondary, tertiary and quaternary structures of these mutants, as assessed by CD, fluorescence and analytical ultracentrifuge techniques, were similar to that of the wild-type enzyme. Initial velocity experiments were performed to derive the various kinetic parameters, which were used to analyse further the free energy change and the coupling energy ($\Delta\Delta G_{int}$) between any two residues. The dissociation constants for Mn^{2+} ($K_{d,Mn}$) of the D141A and F236A mutants were increased by approx. 6- and 65-fold respectively, compared with that of the wild-type enzyme. However, the $K_{d,Mn}$ for the double mutant D141A/F236A was only increased by 150-fold. A coupling energy of -2.12 kcal/mol was obtained for Asp^{141} and Phe^{236}. We suggest that Asp^{141} is involved in the second sphere of the metal-binding network of the enzyme.

Key words: binding energy, coupling energy, malic enzyme, metal-binding site, mutation cycle, pigeon liver.

INTRODUCTION

Cytosolic malic enzyme catalyses the $NADP^+$ and metal (Mn^{2+} or Mg^{2+})-dependent reversible oxidative decarboxylation of L-malate, yielding CO_2 and pyruvate. Our previous studies showed that pigeon liver malic enzyme was oxidized and cleaved by the Cu^{2+}–ascorbate system and Asp^{141} was one of the cleavage sites [1]. Further characterization of the role of Asp^{141} by site-specific mutagenesis confirmed that Asp^{141} was involved in the Mn^{2+}–L-malate binding of the enzyme [2]. Mutation of Asp^{178} (corresponding to Asp^{141} in pigeon enzyme) in *Ascaris* malic enzyme to alanine caused a 50-fold increase of $K_{d,Mg}$ [3]. The crystal structures of malic enzymes from human [4], the nematode *Ascaris suum* [5], and the recently resolved structure of the pigeon enzyme [6] showed that this aspartic residue is a potential second-sphere residue. Asp^{141} is near to Phe^{236}, the amino-acid residue that immediately follows the Mn^{2+} ligands Glu^{234} and Asp^{235}. The length of the side chains between Asp^{141} and Phe^{236} is 3.7 Å (where 1 Å is 0.1 nm). A local change in Asp^{141} might, through Phe^{236}, perturb the orientation of Glu^{234} and Asp^{235} and introduce an indirect effect on the Mn^{2+} binding [2]. The present study is aimed to address the precise interactions between Asp^{141} and Phe^{236}. In order to access all possible interactions, we constructed various double mutants, in which complete mutation cycles, including all non-alanine effects, are considered.

MATERIALS AND METHODS

Site-directed mutagenesis, expression, purification and characterization of the recombinant pigeon liver malic enzymes

Protocols for the site-directed mutagenesis of pigeon liver malic enzyme at Asp^{141} were described previously [2]. The nucleotide sequences used for additional mutations at Phe^{236} were 5′-AGC-ATTAGC**AGC**ATCCTCAAA-3′ for F236A (Phe^{236} → Ala) and 5′-AGCATTAGC**CAG**ATCCTCAAA-3′ for F236L, with the mutational site underlined and in bold. Transformation of wild-type (WT) and mutated plasmids, and purification of the recombinant enzymes were performed as described by Chou et al. [7]. All the mutated cDNAs were also examined by dideoxy chain-termination sequencing [8] to exclude any unexpected mutations that might have resulted from the *in vitro* extension. The absence of adventitious base changes was verified. The recombinant WT malic enzyme has an identical amino-acid sequence and thus has the same physicochemical properties with those of the nature malic enzyme, as characterized previously [7].

Fluorescence spectra of the recombinant malic enzymes were obtained with a PerkinElmer LS 50B luminescence spectrometer at 25 °C. All spectra were corrected for the buffer absorption.

CD measurements were made with a Jasco J-810 spectropolarimeter at 25 °C under constant nitrogen flush, using a 1 mm path-length cell and taking the mean of the ten repetitive

Abbreviation used: WT, wild-type

[1] To whom correspondence should be addressed (e-mail ggchang@ym.edu.tw).

un-smooth scans between 250 and 180 nm. Parallel spectra of urea without protein were also recorded and subtracted from the sample spectra.

Sedimentation velocity experiments were performed using a Beckman XL-A analytical ultracentrifuge. Ultracentrifugation was carried out with a four-hole AnTi60 rotor and double-sector aluminium centrepieces at 40 000 rev./min and 20 °C for 2 h. Data were collected every 2 min and were analysed by the second moment method using Origin 4.1 software provided by Beckman-Coulter to estimate the sedimentation coefficient values.

Enzyme assay

Malic enzyme activity was assayed according to the method described by Chou et al. [9]. Protein concentration was determined by the protein-dye binding method [10]. Apparent Michaelis constants for the substrate and cofactors were determined by varying the concentration of one substrate (or cofactors) around its K_m value and maintaining the other components constant at the saturating level. The kinetic parameters were obtained by fitting the experimental data to appropriate kinetic models in the EZ-FIT program [11].

The above experiment only estimated the apparent kinetic parameters for the substrate and cofactors. To obtain the true kinetic parameters, an initial velocity experiment by varying both Mn^{2+} and L-malate concentrations was performed. The original data were globally fitted to the following equation, which describes a random Bi Bi mechanism in the Mn^{2+} and L-malate binding:

$$v = \frac{V_{max} \cdot [Mal][Mn^{2+}]}{K_{d,Mn} \cdot K_{m,Mal} + K_{m,Mn}[Mal] + K_{m,Mal}[Mn^{2+}] + [Mal][Mn^{2+}]} \quad (1)$$

where v and V_{max} are the observed and maximum velocities respectively, $K_{d,Mn}$, $K_{m,Mn}$ and $K_{m,Mal}$ are the dissociation constant of Mn^{2+}, and the Michaelis constants for Mn^{2+} and L-malate respectively, and [Mal] and [Mn^{2+}] are the concentrations of L-malate and Mn^{2+} respectively. The calculation was carried out with the Sigma Plot 5.0 program (Jandel, San Rafael, CA, U.S.A.).

RESULTS

Purification and characterization of recombinant malic enzymes

The WT and various mutants of malic enzyme were successfully expressed and purified to apparent homogeneity by Q-Sepharose and adenosine-2′,5′-bisphosphate–agarose columns according to our previously published procedures [7]. For the recombinant malic enzymes, the recovery was usually between 50 and 80%. In most cases, a single protein band corresponding to a molecular mass of about 62 kDa was observed following SDS/PAGE for all recombinant malic enzymes (Figure 1). Tiny contaminants were detectable with overloading samples as seen for the WT and D141A mutant enzymes (lanes c, Figure 1). All enzyme samples were estimated to be > 95% pure.

To determine whether or not the mutations affected the overall structural integrity, far-UV CD and fluorescence spectra, as well as the sedimentation coefficient, were measured for all recombinant malic enzymes. In all cases, similar CD spectra were obtained (Figure 2A). All of the recombinant enzymes absorbed UV light with an absorption maximum at 280 nm and the fluorescence emission maximum at 320 nm with the same emission intensity, showing similar conformation for the WT and mutant enzymes (Figure 2B). The WT enzyme sedimented at approx. 10 S (Figure 2C). All other mutants gave similar sedimentation patterns as the WT and yielded sedimentation coefficients of 9.8 $\pm$ 0.3 S indicating similar quaternary structure with the WT enzyme.

Kinetic properties of the recombinant malic enzyme

Preliminary kinetic analysis indicated that the apparent $K_{m,NADP}$ (app) for all mutants was similar to that of the WT enzyme (Table 1). These results suggest that the structural environment of the nucleotide-binding domain is not disturbed by the mutations. The $K_{m,Mn}$ (app) of D141A and D141N were increased by approx. 13- and 23-fold respectively, as compared with the WT enzyme (results not shown). This suggests the perturbation of metal binding as we proposed previously [2]. The $K_{m,Mn}$ (app) of F236A was increased by 75-fold, indicating that the side chain of Phe^{236} is also important in the stabilization of metal binding. The $K_{m,Mn}$ (app) for all double mutants increased by more than 200-fold compared with the WT enzyme. These results give some information about a possible interaction between Asp^{141} and Phe^{236}. The detailed kinetic behaviour of these mutants was then analysed with initial velocity studies to derive the true K_m and K_d values for the metal ion and K_m for L-malate.

The initial velocity experiments showed intersecting patterns for the recombinant malic enzymes (Figure 3). These results indicate that the sequential kinetic mechanism of the enzyme with Mn^{2+} and L-malate was not changed after mutation at the putative metal site. The kinetic parameters of WT and mutant enzymes are summarized in Table 1. The $K_{d,Mal}$ and $K_{m,Mn}$ increased in parallel with mutants at either Asp^{141} or Phe^{236}. The k_{cat} values altered significantly for D141N and D141A/F236A.

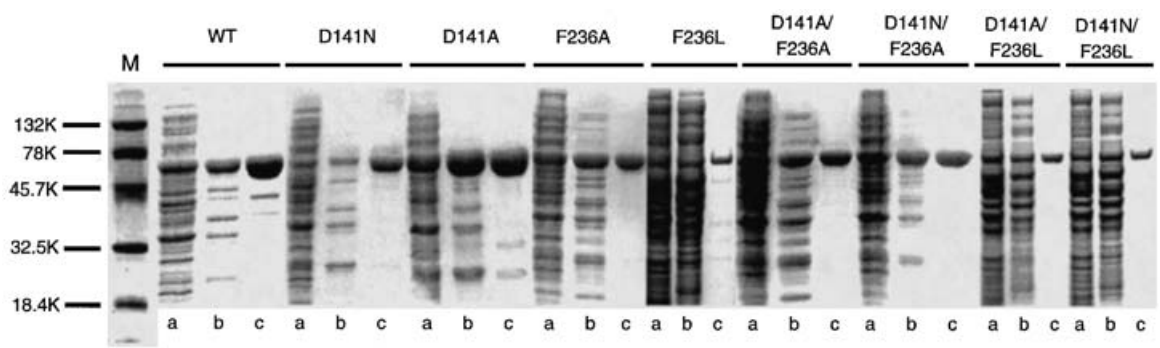

Figure 1 Overexpression and purification of the recombinant pigeon liver malic enzymes

SDS/PAGE was used to examine the expression and purification efficiency. Lane M is the molecular-mass markers (Bio-Rad). Lanes a are those of the crude extract; lanes b are samples from the Q-Sepharose column; lanes c are samples from the affinity column.

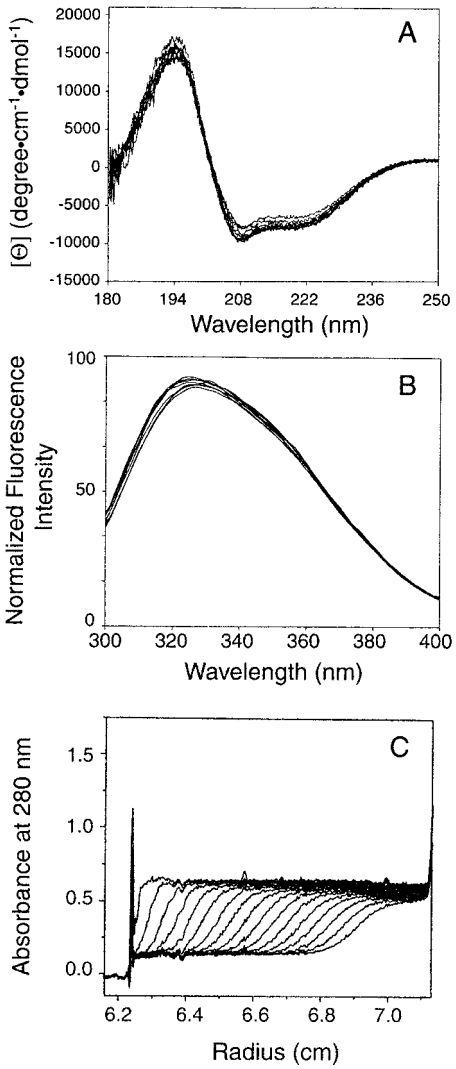

Figure 2 Biophysical characterization of the recombinant pigeon liver malic enzymes

CD spectra (**A**) and fluorescence emission spectra (**B**) were obtained for all recombinant malic enzymes. (**C**) Sedimentation velocity traces of WT enzyme.

The weak binding of the substrate and the metal ion have caused all double mutants to have very small overall catalytic efficiency, $k_{cat}/(K_{d,Mn} \cdot K_{m,NADP} \cdot K_{m,Mal})$. Among them, D141N/F236A decreased by 10^6-fold compared with the WT enzyme, corresponding to 8.1 kcal/mol elevation of the weighted mean activation free energy as estimated by the following relationship [12,13]:

$$\Delta G\ddagger_{mut} = -RT \cdot \ln[(k_{cat,mutant}/K_{m,mutant})/(k_{cat,WT}/K_{m,WT})] \quad (2)$$

where R is the gas constant and T is the absolute temperature.

The D141N/F236A mutant, however, includes a non-alanine mutation at Asp^{141}. Detailed mutation cycles involving all possible combination of mutations at Asp^{141} and Phe^{236} are constructed and analysed.

Interactions between Asp^{141} and Phe^{236} in the metal binding of pigeon liver malic enzyme

Since the mutants do not introduce any major structural change, the differences in free-energy change obtained from the dissociation constants can provide a quantitative estimate for the energy of interaction between the two residues. The free energy change of any mutation (ΔG_{mut}) can be estimated by the following equation:

$$\Delta G_{mut} = -RT \cdot \ln(K_{d,WT}) - [-RT \cdot \ln(K_{d,mut})] = RT \cdot \ln(K_{d,mut}/K_{d,WT}) \quad (3)$$

in which $K_{d,WT}$ and $K_{d,mut}$ are the dissociation constants for WT and mutant enzymes respectively.

Since all the free energies are taken with reference to WT by eqn 3, the coupling energy (ΔG_{int}) between residue A and residue B in the A/B double-mutant cycle is given by:

$$\Delta\Delta G_{int} = \Delta G_{double\ mutant} - (\Delta G_{mutant\ A} + \Delta G_{mutant\ B}) \quad (4)$$

where $\Delta\Delta G_{int}$ measures the co-operative contribution by both A and B. If the effects of the two residues are independent, the coupling energy for the double mutant is the sum of the two single mutants and $\Delta\Delta G_{int}$ will be zero. On the other hand, if there is an interaction between the two residues, the coupling energy for the double mutant is different from the sum of the energies of the two single mutants.

The coupling energies calculated from the four double mutant cycles are shown in Figure 4, which dissected the D141N/F236L double mutant into four double-mutation cycles with alanine as a reference state. The coupling energy of each mutation cycle ($\Delta\Delta G_{int}$) was estimated by eqn 4. The overall coupling energy of the D141N/F236L double mutant ($\Delta\Delta\Delta G_{int}$) related to the four mutation cycles can be estimated by:

$$\Delta\Delta\Delta G_{int} = \Delta\Delta G_{int}(I) - \Delta\Delta G_{int}(II) - \Delta\Delta G_{int}(III) + \Delta\Delta G_{int}(IV) \quad (5)$$

Table 1 Kinetic parameters of the recombinant pigeon liver malic enzymes

Recombinant malic enzyme	$K_{m,NADP}$ (μM)	$K_{m,Mal}$ (mM)	$K_{m,Mn}$ (μM)	$K_{d,Mn}$ (μM)	k_{cat} (s^{-1})	$k_{cat}/(K_{d,Mn} \cdot K_{m,NADP} \cdot K_{m,Mal})$ ($s^{-1} \cdot mM^{-1} \cdot \mu M^{-2}$)
WT	2.6 ± 0.7	0.1 ± 0.01	2.5 ± 0.2	5.1 ± 0.7	87 ± 2.4	66
D141A	4.6 ± 0.6	0.6 ± 0.1	20.3 ± 3.7	29.5 ± 5.0	97 ± 6.4	1.2
D141N	2.5 ± 0.2	0.7 ± 0.07	23.1 ± 1.8	128 ± 16	4.9 ± 0.1	0.02
F236A	4.5 ± 0.7	0.4 ± 0.07	176 ± 15	328 ± 84	71 ± 2.8	0.12
F236L	4.4 ± 0.8	0.2 ± 0.03	8.0 ± 0.6	31.4 ± 6.0	64 ± 1.6	2.3
D141A/F236A	6.1 ± 0.4	3.0 ± 0.4	902 ± 169	642 ± 143	26 ± 2.0	0.002
D141N/F236A	11.6 ± 1.1	22.9 ± 15.1	15 800 ± 10 600	2580 ± 450	59 ± 34	9×10^{-5}
D141A/F236L	4.3 ± 0.3	1.2 ± 0.2	1094 ± 162	660 ± 118	84 ± 5.7	0.025
D141N/F236L	12.5 ± 2.6	3.3 ± 0.4	5075 ± 587	2366 ± 283	149 ± 12	0.0015

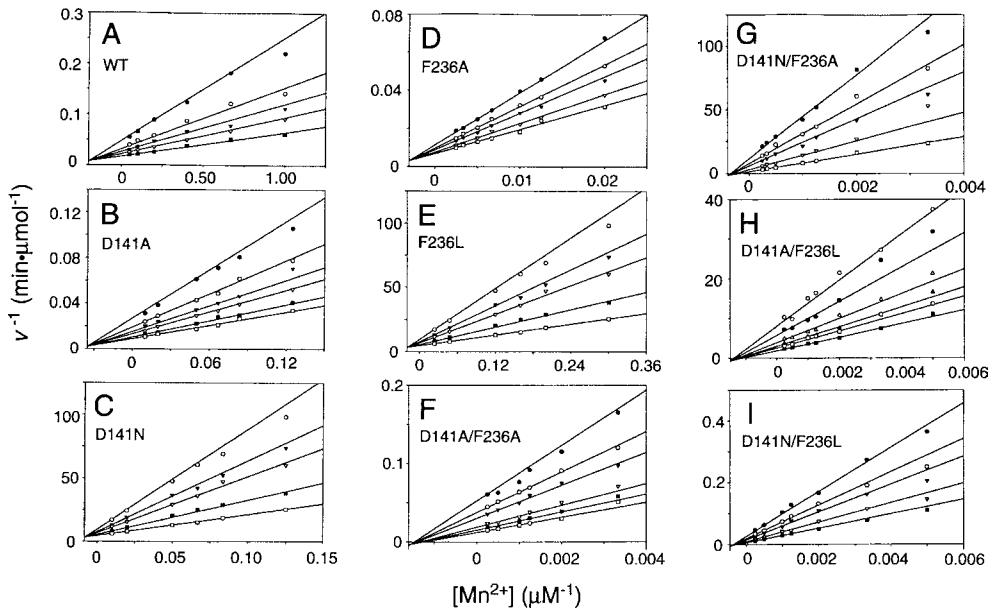

Figure 3 Initial velocity patterns of the recombinant pigeon liver malic enzymes

From top to bottom, the L-malate concentrations were: (**A**) WT, 0.05, 0.1, 0.15, 0.25 and 1 mM; (**B**) D141A, 0.3, 0.5, 0.75, 1.0, 2.0 and 4.0 mM; (**C**) D141N, (**D**) F236A, (**G**) D141N/F236A and (**I**) D141N/F236L, 0.5, 0.75, 1.0, 2.0 and 5.0 mM; (**E**) F236L, 0.2, 0.5, 0.75, 1.0 and 2.0 mM; (**F**) D141A/F236A, 0.5, 0.75, 1.0, 2.0, 3.0 and 5.0 mM; (**H**) D141A/F236L, 0.2, 0.3, 0.5, 0.75, 1.0 and 2.0 mM. The lines represent computer-fitted results according to eqn 1.

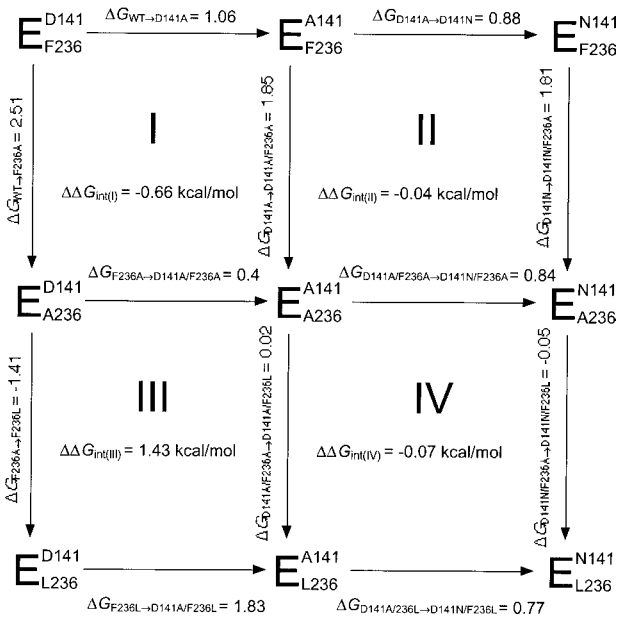

Figure 4 Effect of mutations on the metal binding of malic enzyme analysed by combination of double-mutation cycles between Asp^{141} and Phe^{236}

From WT (D141/F236) to the double mutant D141N/F236L, four mutation cycles were constructed by mutating each or both the residues to alanine first. The free energy changes of each mutation step were calculated from the $K_{d,Mn}$ values. The coupling energy of each mutation cycle is also shown. A positive value indicates hindered Mn^{2+} binding after mutation.

An overall energy of -2.12 kcal/mol was obtained, which indicated strong interactions between Asp^{141} and Phe^{236} residues.

DISCUSSION

Site-directed mutagenesis is a powerful tool in identifying the essential amino-acid groups of enzyme molecules. Alanine screening, which mutates the putative essential amino-acid residues to alanine to eliminate all the side interactions of that residue, is an effective general approach. This procedure, however, ignores the importance of steric effects in protein folding. For a complete investigation, other mutants with replacement of isosteric residues are necessary [14,15]. These, however, might introduce new interactions that could significantly perturb the local structure of the enzyme molecule. Furthermore, the plasticity of the enzyme active site made the interpretation of the mutagenesis results even more complicated [16,17].

The double-mutation cycle has been introduced to explore the interactions between neighbouring groups in an enzyme/protein molecule [13,18–20]. Quantitative interpretation of double mutations of enzymes may provide valuable information about the additive or synergistic effects of the two mutated residues [19]. In a discussion of the 'not-to-alanine' double-mutation cycles, Faiman and Horovitz [21] raised a theoretical consideration on the choice of reference mutant states. In the present paper, we provide experimental data to address the coupling energy corresponding to the not-to-alanine double-mutant cycle.

To understand the energetics of pairwise interactions, we have applied the double-mutant cycle method to study the energetics of interaction between Asp^{141} and Phe^{236}. We generated four double-mutant cycles to identify the possible interactions between Asp^{141} and Phe^{236}. Through this kind of interaction, Asp^{141} was found to be involved in the Mn^{2+}–L-malate binding of the pigeon liver malic enzyme.

The $\Delta\Delta G_{int}$ for the D141N/F236L double mutation accounts for -2.12 kcal/mol, which is larger than that expected for the van der Waals contact (0.4–0.7 kcal/mol) [22]. Asp^{141} may protonate in the interior of the enzyme molecule. In that case, an induced dipole-induced dipole π–π interaction between the carboxy group and the aromatic phenyl group is anticipated. More recently, the CH–π or cation–π interactions have raised much attention [23,24]. The dihedral angle of the planes between adjacent aromatic rings or of the histidine ring interacting with aromatic residues is significantly non-random. On the contrary, the dihedral

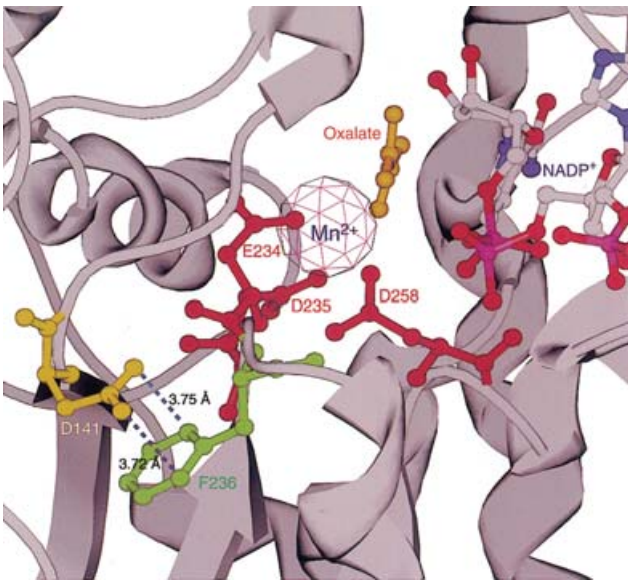

Figure 5 Crystal structure of pigeon liver malic enzyme at the active centre region

The closed form of pigeon liver malic enzyme (Protein Data Bank code 1GQ2) is shown with the focus on the metal-binding region. The stacking between Asp^{141} and Phe^{236} is highlighted with broken lines. This image was generated with Spock and rendered with Raster3D [26].

angle of carboxyl groups with other planar groups is randomly distributed [25]. On a statistical basis, 73% of the interplanar organization of a carboxy side chain with phenyl rings tends to establish orthogonal planes in a side-by-side position. However, the carboxy plane of Asp^{141} and the aromatic plane of Phe^{236} in malic enzyme are almost parallel to each other (Figure 5). A π–π stacking interaction might have an important role in maintaining the structural integrity around the active centre.

Examination of the metal site of pigeon malic enzyme reveals that the metal ligands Glu^{234}, Asp^{235}, Asp^{258}, oxalate and other essential amino-acid residues all reside within the van der Waals contact (< 4 Å) from Mn^{2+} [6,12]. Asp^{141} is 11 Å away from Mn^{2+}. Furthermore, besides Phe^{236}, there are many highly conserved hydrophobic amino-acid residues, i.e. Val^{138}, Val^{139}, Met^{156}, Phe^{255}, Ile^{145}, Ile^{158} and Pro^{159}, which are within 6–8 Å of the metal centre. Therefore a more plausible structural basis for keeping the metal site intact would be by considering the Phe^{236} as one of the components of the hydrophobic core that isolate the polar active centre from other parts of the structure and ensure an optimal environment for binding and catalysis. In this regard, it is conceivable that the substitution of leucine for Phe^{236} (F236L) restores most of the binding energy (1.41 kcal/mol) lost in F236A (2.51 kcal/mol) (Table 1 and Figure 4). Indeed, among the 33 malic enzyme sequences available, 27 had phenylalanine, in other cases either isoleucine or leucine, at position 236. The hydrophobic characteristic in the microenvironment of Phe^{236} seems to be essential for malic enzyme to have a proper metal-binding environment.

This work was supported by the National Science Council, Republic of China (Frontiers in Sciences Program, NSC 90-2321-B010-006).

Received 18 February 2003/9 June 2003; accepted 19 June 2003
Published as BJ Immediate Publication 19 June 2003, DOI 10.1042/BJ20030268

REFERENCES

1 Chou, W. Y., Tsai, W. P., Lin, C. C. and Chang, G. G. (1995) Selective oxidative modification and affinity cleavage of pigeon liver malic enzyme by the Cu^{2+}–ascorbate system. J. Biol. Chem. **270**, 25935–25941
2 Chou, W. Y., Chang, H. P., Huang, C. H., Kuo, C. C., Tong, L. and Chang, G. G. (2000) Characterization of the functional role of Asp141, Asp194, and Asp464 residues in the Mn^{2+}–L-malate binding of pigeon liver malic enzyme. Protein Sci. **9**, 242–251
3 Karsten, W. E., Chooback, L., Liu, D., Hwang, C. C., Lynch, C. and Cook, P. F. (1999) Mapping the active site topography of the NAD-malic enzyme via alanine-scanning site-directed mutagenesis. Biochemistry **38**, 10527–10532
4 Xu, Y., Bhargava, G., Wu, H., Loeber, G. and Tong, L. (1999) Crystal structure of human mitochondrial $NAD(P)^+$-dependent malic enzyme: a new class of oxidative decarboxylases. Structure **7**, 877–889
5 Coleman, D. E., Rao, G. S., Goldsmith, E. J., Cook, P. F. and Harris, B. G. (2002) Crystal structure of the malic enzyme from *Ascaris suum* complexed with nicotinamide adenine dinucleotide at 2.3 Å resolution. Biochemistry **41**, 6928–6938
6 Yang, Z., Zhang, H., Hung, H. C., Kuo, C. C., Tsai, L. C., Yuan, H. S., Chou, W. Y., Chang, G. G. and Tong, L. (2002) Structural studies of the pigeon cytosolic NADP-dependent malic enzyme. Protein Sci. **11**, 332–341
7 Chou, W. Y., Huang, S. M. and Chang, G. G. (1997) Functional roles of the N-terminal amino acid residues in the Mn(II)–L-malate binding and subunit interactions of pigeon liver malic enzyme. Protein Eng. **10**, 1205–1211
8 Sanger, F., Nicklen, S. and Coulson, A. R. (1997) DNA sequencing with chain-terminating inhibitors. Proc. Natl. Acad. Sci. U.S.A. **74**, 5463–5467
9 Chou, W. Y., Huang, S. M., Liu, Y. H. and Chang, G. G. (1994) Cloning and expression of pigeon liver cytosolic $NADP^+$-dependent malic enzyme cDNA and some of its abortive mutants. Arch. Biochem. Biophys. **310**, 158–166
10 Bradford, M. M. (1976) A rapid and sensitive method for the quantitation of microgram quantities of protein utilizing the principle of protein-dye binding. Anal. Biochem. **72**, 248–254
11 Perrella, F. W. (1988) EZ-FIT: a practical curve-fitting microcomputer program for the analysis of enzyme kinetic data on IBM-PC compatible computers. Anal. Biochem. **174**, 437–447
12 Wells, J. A. (1990) Additivity of mutational effects in proteins. Biochemistry **29**, 8509–8517
13 Di Cera, E. (1998) Site-specific analysis of mutational effects in proteins. Adv. Protein Chem. **51**, 59–119
14 Plapp, B. V. (1995) Site-directed mutagenesis: a tool for studying enzyme catalysis. Methods Enzymol. **249**, 91–119
15 Fersht, A. R. (1999) Protein engineering. In Structure and Mechanism in Protein Science: a Guide to Enzyme Catalysis and Protein Folding, pp. 420–456, Freeman, New York
16 Peracchi, A. (2001) Enzyme catalysis: removing chemically 'essential' residues by site-directed mutagenesis. Trends Biochem. Sci. **26**, 497–503
17 Todd, A. E., Orengo, C. A. and Thornton, J. M. (2002) Plasticity of enzyme active sites. Trends Biochem. Sci. **27**, 419–426
18 Carter, P. J., Winter, G., Wilkinson, A. J. and Fersht, A. R. (1984) The use of double mutants to detect structural changes in the active site of the tyrosyl-tRNA synthetase (*Bacillus stearothermophilus*). Cell **38**, 835–840
19 Mildvan, A. S., Weber, D. J. and Kuliopulos, A. (1992) Quantitative interpretations of double mutations of enzymes. Arch. Biochem. Biophys. **294**, 327–340
20 Di Cera, E. (1998) Site-specific thermodynamics: understanding cooperativity in molecular recognition. Chem. Rev. **98**, 1563–1592
21 Faiman, G. A. and Horovitz, A. (1996) On the choice of reference mutant states in the application of the double-mutant cycle method. Protein Eng. **9**, 315–316
22 Goldman, E. R., Dall'Acqua, W., Braden, B. C. and Mariuzza, R. A. (1997) Analysis of binding interactions in an idiotope-antiidiotope protein–protein complex by double mutant cycles. Biochemistry **36**, 49–56
23 Brandl, M., Weiss, M. S., Jabs, A., Suhnel, J. and Hilgenfeld, R. (2001) C-H $\cdots$ π-interactions in proteins. J. Mol. Biol. **307**, 357–377
24 Ma, J. C. and Dougherty, D. A. (1997) The cation–π interaction. Chem. Rev. **97**, 1303–1324
25 Brocchieri, L. and Karlin, S. (1994) Geometry of interplanar residue contacts in protein structures. Proc. Natl. Acad. Sci. U.S.A. **91**, 9297–9301
26 Merrit, E. A. and Bacon, D. J. (1997) Raster3D: photorealistic molecular graphics. Methods Enzymol. **277**, 505–524